

## An Unconditionally Stable Scheme for the Shallow Water Equations\*

MOSHE ISRAELI

*Computer Science Department, Technion, Haifa, Israel*

NAOMI H. NAIK AND MARK A. CANE

*Lamont-Doherty Earth Observatory, Columbia University, Palisades, New York*

(Manuscript received 24 September 1998, in final form 1 March 1999)

### ABSTRACT

A finite-difference scheme for solving the linear shallow water equations in a bounded domain is described. Its time step is not restricted by a Courant–Friedrichs–Levy (CFL) condition. The scheme, known as Israeli–Naik–Cane (INC), is the offspring of semi-Lagrangian (SL) schemes and the Cane–Patton (CP) algorithm. In common with the latter it treats the shallow water equations implicitly in  $y$  and with attention to wave propagation in  $x$ . Unlike CP, it uses an SL-like approach to the zonal variations, which allows the scheme to apply to the full primitive equations. The great advantage, even in problems where quasigeostrophic dynamics are appropriate in the interior, is that the INC scheme accommodates complete boundary conditions.

### 1. Introduction

The two-dimensional linearized shallow water equations represent the evolution of small perturbations in the flow field of a shallow basin on a rotating sphere. Our interest in these model equations arises from our interest in solving for the motions in a linear beta-plane deep ocean. If the stratification is assumed to be purely a function of depth, then the solution can be found as a sum over  $N$  vertically standing normal modes, each of which satisfies a shallow water system. Moreover, this is the wave operator even in nonlinear problems and is used in both semi-Lagrangian and semiimplicit schemes. For example, it could readily be used in the standard semiimplicit setup as the solution procedure for the wave operator.

Two successful, but very different, approaches to solving the shallow water system are standard leapfrog with centered space differences and the Cane–Patton (CP; Cane and Patton 1984) scheme. The leapfrog scheme is the standard explicit time-stepping scheme used routinely for generic advection problems. As for all explicit schemes, a Courant–Friedrichs–Levy (CFL) condition restricts the allowed time step, but the scheme

is easy to code and boundary conditions for the discretized equations are fairly natural to impose. At the other end of the spectrum, the CP algorithm is specifically designed with the characteristics of the physics of the equatorial ocean dynamics in mind. By separating the free modes into the eastward propagating Kelvin mode and the remaining westward propagating modes, the shallow water system can be solved semiimplicitly with very large time steps. The major drawback to this approach is that it is prohibitively awkward to treat realistic boundaries.

Here we present a new scheme that has neither of the disadvantages of these schemes: it is not restricted by a CFL condition nor are there restrictions on the basin geometry. The unconditional stability of the scheme means that only accuracy, not computational stability, determines an appropriate time step. Since the time step in present ocean circulation codes is restricted by the CFL associated with inertia-gravity waves of no importance for the large-scale ocean circulation, this is potentially of great value.

The new scheme, Israeli–Naik–Cane (INC), combines concepts from semi-Lagrangian (SL) methods (e.g., Staniforth and Côté 1991) and the CP scheme. It is entirely natural to envision solving a tracer equation,  $dC/dt = 0$ , at a point  $\mathbf{x}$  and time  $t$  by following a characteristic back to a “take-off point”  $\mathbf{x}_*$  at the previous time  $t - \Delta t$ . Here SL extends this strategy to nonpassive quantities such as momentum and pressure. In doing so for a shallow water system, SL is applied only to the advective operator, which is split off from the wave

\* Lamont-Doherty Earth Observatory Contribution Number 6014.

*Corresponding author address:* Dr. Naomi Naik, Lamont-Doherty Earth Observatory, Columbia University, 106 D Oceanography, Palisades, NY 10964.  
E-mail: naomi@lamont.ldeo.columbia.edu

operator. The latter is usually solved implicitly. The SL method thus does not follow the true characteristics of the system. In the INC scheme we first split off the zonal direction part of the wave operator and treat it in a semi-Lagrangian manner, and then, as in CP, solve the meridional part implicitly. INC somewhat resembles the method of bicharacteristics (e.g., Roe 1994), the important difference being this implicit step. In INC, as in CP, the different treatment of the  $x$  and  $y$  directions is motivated by the anisotropy of planetary waves on a rotating sphere (on a beta plane); that is, they propagate in the  $x$  direction but are standing in the  $y$  direction.

**2. Method**

The nondimensional linearized shallow water system in two space dimensions can be written as

$$\partial_t u - fv + \partial_x h = F \tag{1}$$

$$\partial_t v + fu + \partial_y h = G \tag{2}$$

$$\partial_t h + \partial_x u + \partial_y v = Q, \tag{3}$$

where a partial derivative with respect to  $x$ , for example, is denoted as  $\partial_x$ . The variables  $u$ ,  $v$ ,  $h$ , and forcings  $F$ ,  $G$ , and  $Q$  are all functions of  $x$ ,  $y$ , and  $t$ . The remaining symbol is  $f$ , the nondimensional coriolis parameter, which is a function of  $y$  (latitude), only. The dimensional equations and variables can be recovered by multiplying  $h$  by  $H$ ,  $(u, v)$  by  $U$ ,  $t$  by  $T$ , and  $(x, y)$  by  $L$ , where  $U = c$ ,  $H = c^2/g$ ,  $T = (c\beta)^{-1/2}$ , and  $L = (c/\beta)^{1/2}$ . The dimensional forcing terms are  $(U/T)F$ ,  $(U/T)G$ , and  $(H/T)Q$ .

To solve an initial value problem satisfying this system analytically, we specify the solution  $(u, v, h)$  at a beginning time,  $t_0$ , and find an expression for  $(u, v, h)$  for all  $t > t_0$ . Numerically, we usually employ a time-stepping scheme, where we specify an algorithm for advancing the solution from any time  $t - \Delta t$  to a time  $t$ . Thus, assuming a uniform grid in time, this algorithm is just a recurrence relation for the solution at  $t = t^{n+1}$ , given the solution at  $t = t^n$ , where  $t^i = t_0 + i\Delta t$ .

The motivation for the INC scheme comes from the observation that, if  $v$  were known, then Eqs. (1) and (3) form a hyperbolic system, which is easily diagonalized, with characteristics given by lines of constant  $x - t$  and  $x + t$  with characteristic variables,  $u + h$  and  $u - h$ . This is easy to see by simply adding and subtracting (1) and (3), yielding

$$(\partial_t + \partial_x)(u + h) = fv - \partial_y v + F + Q$$

$$(\partial_t - \partial_x)(u - h) = fv + \partial_y v + F - Q.$$

For each fixed latitude line, that is,  $y = \text{constant}$ , these two decoupled equations propagate the quantities  $u + h$  and  $u - h$  in opposite directions along characteristics in  $(x, t)$  space with unit speed. Solving these equations is straightforward: the right-hand sides are integrated

along the lines of constant  $x - t$  and  $x + t$ , respectively, that is,

$$(u + h)(x, t) = (u + h)(x - \Delta t, t - \Delta t) + \int_0^{\Delta t} (fv - \partial_y v + F + Q)(x - s, t - s) ds$$

$$(u - h)(x, t) = (u - h)(x + \Delta t, t - \Delta t) + \int_0^{\Delta t} (fv + \partial_y v + F - Q)(x + s, t - s) ds.$$

These two equations can be combined to easily find  $u(x, t)$  and  $h(x, t)$  given  $u$  and  $h$  at the previous time and  $v$  and  $\partial_y v$  for time in the interval  $(t - \Delta t, t)$ .

To solve the problem, we must relax the assumption of knowing  $v$  (and  $\partial_y v$ ) for a whole time interval. We approximate the integrals along characteristics, assuming we know  $v$  at the beginning of the time step,  $t = t^n$ , and at the end of the time step,  $t = t^{n+1}$ . The trapezoidal rule yields a second-order approximation of the integrals, and gives us the following formulas for  $u + h$  and  $u - h$  at the new time step:

$$(u + h)^{n+1} = (u + h)_L^n + \tau[(fv - \partial_y v + F + Q)^{n+1} + (fv - \partial_y v + F + Q)_L^n] \tag{4}$$

$$(u - h)^{n+1} = (u - h)_R^n + \tau[(fv + \partial_y v + F - Q)^{n+1} + (fv + \partial_y v + F - Q)_R^n], \tag{5}$$

where quantities without subscripts are evaluated at an arbitrary grid point,  $(x, y)$ , with a subscript ‘‘R,’’ they are evaluated at  $(x + \Delta t, y)$ , and with a subscript ‘‘L,’’ at  $(x - \Delta t, y)$ . Superscripts  $n$  and  $n + 1$  indicate quantities at  $t^n$  and  $t^{n+1}$ , respectively. For convenience,  $\tau = \Delta t/2$ .

These explicit formulas for  $u^{n+1}$  and  $h^{n+1}$  depend on  $v^{n+1}$ . To compute  $v^{n+1}$ , we discretize the  $y$ -momentum equation (2) in time using a centered, second-order scheme:

$$\frac{v^{n+1} - v^n}{\Delta t} + \frac{\partial_y h^{n+1} + \partial_y h^n}{2} + f \frac{u^{n+1} + u^n}{2} = \frac{G^{n+1} + G^n}{2}. \tag{6}$$

Suppressing the superscript for quantities at time  $t^{n+1}$  and rearranging terms with known quantities on the right, unknown on the left:

$$v + \tau(\partial_y h + fu) = v^n - \tau(\partial_y h^n + fu^n - G - G^n). \tag{7}$$

To decouple Eqs. (4), (5), and (7), we solve Eqs. (4) and (5) for  $u^{n+1}$  and  $h^{n+1}$ , and substitute into Eq. (7). Solving for  $u$  and  $h$  (again suppressing the superscript for quantities at time  $t^{n+1}$ ), gives

$$u = \tau f v + c^n \tag{8}$$

$$h = -\tau \partial_y v + d^n, \tag{9}$$

where

$$c^n = \frac{1}{2} \{ (u + h)_L^n + (u - h)_R^n + \tau [2F + (fv - \partial_y v + F + Q)_L^n + (fv + \partial_y v + F - Q)_R^n] \}$$

$$d^n = \frac{1}{2} \{ (u + h)_L^n - (u - h)_R^n + \tau [2Q + (fv - \partial_y v + F + Q)_L^n - (fv + \partial_y v + F - Q)_R^n] \}.$$

Substituting these formulas into the  $y$  momentum equation (7), and rearranging terms,

$$\begin{aligned} & \partial_y^2 v - \left( \frac{1}{\tau^2} + f^2 \right) v \\ &= \frac{1}{\tau} [fu^n + fc^n + \partial_y(h^n + d^n) - (G + G^n)] \\ & \quad - \frac{1}{\tau^2} v^n. \end{aligned} \tag{10}$$

This formula for  $v$  is simply a second-order ordinary differential equation (ODE) in  $y$ . Once we have found  $v$ , we obtain  $u$  and  $h$  using Eqs. (8) and (9). To complete the description of the scheme, we need discretizations of  $\partial_y v$  and  $\partial_y^2 v$ . On an A-grid, where  $u$ ,  $v$ , and  $h$  are defined at the same grid points, second-order approximations to  $\partial_y v$  and  $\partial_y^2 v$  are defined as

$$\partial_y v \approx \delta_y v \stackrel{\text{def}}{=} \frac{1}{2\Delta y} (v_{i,j+1} - v_{i,j-1}) \quad \text{and}$$

$$\partial_y^2 v \approx \delta_{yy} v \stackrel{\text{def}}{=} \frac{1}{\Delta y^2} (v_{i,j+1} - 2v_{i,j} + v_{i,j-1}).$$

To summarize, the solution algorithm is the following.

**Time-stepping algorithm—Interior points**

0. Assume  $u^n$ ,  $v^n$ ,  $h^n$  are known.

1. Find  $c^n$  and  $d^n$ :

$$c^n = \frac{1}{2} (I_1 + I_2) + \tau F,$$

$$I_1 = (u + h)_L^n + \tau (fv - \partial_y v + F + Q)_L^n$$

$$d^n = \frac{1}{2} (I_1 - I_2) + \tau Q,$$

$$I_2 = (u - h)_R^n + \tau (fv + \partial_y v + F - Q)_R^n.$$

2. Find  $v = v^{n+1}$  by solving an ODE in  $y$  for each value of  $x$ :

$$\begin{aligned} & \delta_{yy} v - \left( \frac{1}{\tau^2} + f^2 \right) v \\ &= \frac{1}{\tau} [fu^n + fc^n + \delta_y(h^n + d^n) - (G + G^n)] - \frac{1}{\tau^2} v^n. \end{aligned}$$

3. Compute  $\delta_y v$ .

4. Find  $u = u^{n+1}$  and  $h = h^{n+1}$ :

$$u = \tau f v + c^n \quad h = -\tau \delta_y v + d^n.$$

Note that, for the discretization in the  $x$  direction, the “take-off” or “departure” points,  $x_{ij} + \Delta t$  and  $x_{ij} - \Delta t$ , do not necessarily fall on grid points. Piecewise cubic interpolation in  $x$  is used to obtain the expressions that need to be evaluated at these points, ensuring that this step does not introduce an instability (Staniforth and Côté 1991). Note that the scheme is computationally undemanding. All steps are explicit except for the solution of the one-dimensional equation in step 1. For a second-order approximation, that may be accomplished with a tridiagonal solve (pentadiagonal for fourth order).

**3. Boundary conditions**

To be relevant to the ocean, we need to solve the shallow water system on a bounded domain. The interior algorithm is easily modified to incorporate no-flow boundary conditions. The boundary condition  $v = 0$  is used at northern and southern boundary points in Eq. (10). In addition,  $\delta_y(d^n)$  must be known at the point next to the boundary, so  $\delta_y v$  is needed at the boundary. This is obtained by a second-order one-sided approximation, consistent with conservation. At the eastern and western boundaries, the simplest algorithm is derived by specifying  $u$  and using only the outgoing characteristic to obtain  $h$ . At the eastern boundary, for example, there is only the characteristic from the left, which determines the boundary condition on  $u + h$ . Assuming no normal flow at the boundary,  $u = 0$ , which then gives a formula for  $h$  directly.

**Time-stepping algorithm—**

**Modifications at boundary points**

**Western boundary points**

1W. Find  $d^n$ :

$$\begin{aligned} d^n &= -(u - h)_R^n \\ & \quad - \tau [F - Q + (fv + \delta_y v + F - Q)_R^n]. \end{aligned}$$

2W. Find  $v = v^{n+1}$  by solving an ODE in  $y$  for each value of  $x$ :

$$\begin{aligned} & \delta_{yy} v + \delta_y(fv) - \frac{1}{\tau^2} v \\ &= \frac{1}{\tau} [\delta_y(d^n + h^n) - (G + G^n)] - \frac{1}{\tau^2} v^n. \end{aligned}$$

4W. Find  $u = u^{n+1}$  and  $h = h^{n+1}$ :

$$u = 0, \quad h = -\tau(fv + \delta_y v) + d^n.$$

Eastern boundary points

1E. Find  $d^n$ :

$$d^n = (u + h)_L^n + \tau[F + Q + (fv - \delta_y v + F + Q)_L^n].$$

2E. Find  $v = v^{n+1}$  by solving an ODE in  $y$  for each value of  $x$ :

$$\begin{aligned} \delta_{yy} v - \delta_y(fv) - \frac{1}{\tau^2} v \\ = \frac{1}{\tau} [\delta_y(d^n + h^n) - (G + G^n)] - \frac{1}{\tau^2} v^n. \end{aligned}$$

4E. Find  $u = u^{n+1}$  and  $h = h^{n+1}$ :

$$u = 0, \quad h = \tau(fv - \delta_y v) + d^n.$$

For grid points near boundaries, and for  $\Delta t > \Delta x$ , an “R” or “L” point can fall outside of the boundary. In this case, the characteristic is traced back in time to when it crossed the boundary. The values of  $u$ ,  $v$ , and  $h$  are not known at this intermediate time,  $\hat{t}$ , so we do a constant extrapolation from the values at the point on the boundary at time  $t^n$ . We also tried a linear extrapolation from the values at times  $t^n$  and  $t^{n-1}$ , and even added a “correction” step, using the linearly extrapolated version as a “predictor,” but after many numerical experiments, concluded that the constant in time extrapolation was sufficient. See appendix A for details and formulas.

#### 4. Conservation

Assuming conservative boundary condition on  $v$  consistent with the closed boundary condition at the northern and southern boundaries of the domain, the new scheme conserves mass in a semiperiodic domain. For a domain with east–west boundaries, the boundary condition given above, which follows a single characteristic into the domain, is nonconservative. Conservative boundary conditions can also be used. For  $\Delta t = \Delta x$ , these can be written as the following.

Time-stepping algorithm—  
Conservative boundary conditions

Western boundary points

1Wc. Find  $c^n$  and  $d^n$ :

$$\begin{aligned} c^n &= 0, \\ I_0 &= (u - h)^n + \tau(fv + \delta_y v + F - Q)^n \\ d^n &= \frac{-1}{2}(I_0 + I_2) + \tau Q, \\ I_2 &= (u - h)_R^n + \tau(fv + \delta_y v + F - Q)_R^n. \end{aligned}$$

2Wc. Find  $v = v^{n+1}$  by solving an ODE in  $y$  for each value of  $x$ :

$$\begin{aligned} \delta_{yy} v - \left( \frac{1}{\tau^2} + f^2 \right) v \\ = \frac{1}{\tau} [fu^n + fc^n + \delta_y(h^n + d^n) - (G + G^n)] \\ - \frac{1}{\tau^2} v^n. \end{aligned}$$

4Wc. Find  $u = u^{n+1}$  and  $h = h^{n+1}$ :

$$u = 0, \quad h = -\tau \delta_y v + d^n.$$

Eastern boundary points

1Ec. Find  $c^n$  and  $d^n$ :

$$\begin{aligned} c^n &= 0, \\ I_0 &= (u + h)^n + \tau(fv - \delta_y v + F + Q)^n \\ d^n &= \frac{1}{2}(I_0 + I_2) + \tau Q, \end{aligned}$$

$$I_2 = (u + h)_L^n + \tau(fv - \delta_y v + F + Q)_L^n.$$

2Ec. Find  $v = v^{n+1}$  by solving an ODE in  $y$  for each value of  $x$ :

$$\begin{aligned} \delta_{yy} v - \left( \frac{1}{\tau^2} + f^2 \right) v \\ = \frac{1}{\tau} [fu^n + fc^n + \delta_y(h^n + d^n) - (G + G^n)] \\ - \frac{1}{\tau^2} v^n. \end{aligned}$$

4Ec. Find  $u = u^{n+1}$  and  $h = h^{n+1}$ :

$$u = 0, \quad h = \tau \delta_y v + d^n.$$

#### 5. Accuracy and stability

In this section, we compare the analytic dispersion relation for the shallow water equations on an equatorial  $\beta$ -plane (with boundary condition:  $u$ ,  $v$ ,  $h$  bounded as  $y \rightarrow \pm\infty$ ), with the numerical dispersion relation of the scheme. Suppose  $u = \tilde{u}e^{i(kx - \omega t)}$ ,  $v = \tilde{v}e^{i(kx - \omega t)}$ , and  $h = \tilde{h}e^{i(kx - \omega t)}$ .

The analytic dispersion relation is most easily obtained by recalling that a single equation for  $v$  may be derived from the nondimensional shallow water equations:

$$(\partial_x^2 v + \partial_y^2 v)_t - f^2 v_t - v_{ttt} + v_x = 0.$$

Using  $v = \tilde{v}e^{i(kx - \omega t)}$ , this equation becomes

$$\partial_y^2 \tilde{v} + \left( \omega^2 - k^2 - \frac{k}{\omega} - f^2 \right) \tilde{v} = 0.$$

Note that, due to our scaling, since  $f = T\hat{f} = Tf_0 + (T\beta L)y$ , then  $df/dy = 1$ . On an equatorial  $\beta$ -plane,  $f_0 = 0$ , and the nondimensional dispersion relation is

$$\omega^2 - k^2 - \frac{k}{\omega} = 2n + 1, \quad n = 0, 1, \dots \quad (11)$$

where the boundary conditions ( $\tilde{v} \rightarrow 0$  as  $y \rightarrow \pm\infty$ ) imply that eigensolutions  $\hat{\Psi}_n$  of the  $\tilde{v}$  equation satisfy

$$(y^2 - \partial_y^2)\hat{\Psi}_n = (2n + 1)\hat{\Psi}_n.$$

For the special case of the Kelvin wave,  $v = 0$ , the dispersion relation is

$$\omega = k, \quad (12)$$

which, for convenience, can be thought of as a special case of Eq. (11) with  $n = -1$ .

As a generalization to the bounded domain, the eigenfunctions of the  $\tilde{v}$  equation satisfy

$$(f^2 - \delta_y^2)\tilde{v} = \mu\tilde{v},$$

see, for example, Cane and Sarachik (1979). The dispersion relation above becomes, after multiplication by  $\omega$ :

$$\omega^3 - k^2\omega - k = \mu\omega. \quad (13)$$

Neutral solutions of the assumed form exist only if the solutions of the cubic are all real; otherwise, there will be a conjugate pair of solutions implying growing and decaying waves. There will be three real roots if the discriminant

$$D(\mu) = \frac{k^2}{4} - \frac{(k^2 + \mu)^3}{27} \quad (14)$$

is not positive. We note that  $\mu > 0$  is required to avoid instability as  $k \rightarrow 0$ . For  $\mu \geq 1.5$  a maximum is obtained at the left end point,  $k = 0$ , of the interval of interest and it is negative, implying stability for all  $k$ . For  $0 \leq \mu \leq 1.5$ , an interior maximum is obtained, of magnitude  $(1 - \mu)/4$ . Thus we may conclude that a necessary and sufficient condition for stability at all wavenumbers is  $\mu \geq 1$ .

Another approach that goes over to the discrete case, gives a proof of sufficiency. Observe that, when  $\mu = 1$ , the discriminant factors as

$$D(1) = -(1 - 2k^2)^2(4 + k^2)/108.$$

Thus  $D(1)$  vanishes for  $k^2 = 1/2$  and is negative elsewhere. Furthermore

$$D(1) - D(\mu) \geq 0$$

for  $\mu \geq 1$  so that the last inequalities are sufficient for stability.

Some of the above steps can be applied to obtain the numerical dispersion relation. Define  $\eta = e^{-i\gamma}$ , and  $\alpha = e^{-i\theta}$ , where  $\gamma = \omega\Delta t$  and  $\theta = k\Delta x$ . Then, if  $\Delta t$  is a multiple of  $\Delta x$ , no interpolation is needed in the  $x$ -direction, and

$$(\eta - \alpha)(\tilde{u} + \tilde{h}) = \tau(\eta + \alpha)(f - \partial_y)\tilde{v}$$

$$(\eta - \alpha^{-1})(\tilde{u} - \tilde{h}) = \tau(\eta + \alpha^{-1})(f + \partial_y)\tilde{v}$$

$$(\eta - 1)\tilde{v} + \tau(\eta + 1)(\partial_y\tilde{h} + f\tilde{u}) = 0.$$

Solving for  $\tilde{u}$  and  $\tilde{h}$  in the first two equations, substituting into the third, using  $\partial f/\partial y = 1$  and  $\mu\tilde{v}$  for  $(f^2 - \delta_y^2)\tilde{v}$  gives the numerical dispersion relation for the scheme:

$$\frac{1}{\tau^2} \left( \frac{\eta - 1}{\eta + 1} \right) (\eta^2 - 2\eta \cos\theta + 1) + \mu(\eta^2 - 1) + 2i\eta \sin\theta = 0, \quad (15)$$

or, dividing through by  $2i\eta$ :

$$\frac{1}{\tau^2}(\cos\gamma - \cos\theta) \tan\frac{\gamma}{2} + \mu \sin\gamma + \sin\theta = 0. \quad (16)$$

As in the continuous case, the special case of the Kelvin wave,  $v = 0$ , has a separate dispersion relation, since solving for  $\tilde{u}$  and  $\tilde{h}$  in the first two equations implies that  $\tilde{u} = \tilde{h} = 0$  unless

$$\gamma = \theta. \quad (17)$$

For convenience, as in the analytic case, we can treat this solution as special case of Eq. (16) with  $\mu = -1$ . However, we must remember that  $\mu = -1$  is *not* an eigenvalue of the operator  $(f^2 - \delta_y^2)\tilde{v}$ , and this case must be analyzed separately.

We would like to find conditions under which the scheme is stable for all values of  $\Delta t$  by deriving a cubic equation for  $g = \tan(\gamma/2)$ , and finding when all three roots are real, in which case  $|\eta| = 1$ . First note that the discrete Kelvin wave solution,  $\mu = -1$ , is stable. So we consider only values of  $\mu$  corresponding to eigenvalues of the discrete operator  $(f^2 - \delta_y^2)\tilde{v}$ .

Using also  $s = \tan(\theta/2)$ ,  $\hat{\tau} = \tau^2$ , and  $\hat{\mu} = \mu\tau^2$  gives rise to

$$g^3 - \hat{\tau}sg^2 - [s^2 + \hat{\mu}(1 + s^2)]g - \hat{\tau}s = 0. \quad (18)$$

We compute the discriminant of the cubic,  $D(\hat{\mu})$ . Setting, without loss of generality,  $\hat{\mu} = \hat{\tau}(1 + 2\hat{n})$ , we get  $\hat{\mu} = \hat{\tau}$  for  $\hat{n} = 0$ . Then like the continuum case the discriminant factors:

$$D(\hat{\tau}) = -[(2 + \hat{\tau})s^2 - \hat{\tau}^2][4\hat{\tau} + (1 + \hat{\tau})^2s^2]/108;$$

this quantity vanishes for  $s^2 = \hat{\tau}^2/(2 + \hat{\tau})$  and is negative elsewhere.

For  $\hat{n} \neq 0$  the discriminant is a complicated expression difficult to evaluate but we observe that the difference  $D(\hat{\tau}) - D(\hat{\mu})$  is a cubic in  $\hat{n}$  and the coefficients of all powers of  $\hat{n}$  are positive, thus  $D(\hat{\mu})$  is negative for positive  $\hat{n}$ , in agreement with the continuous case. Thus a sufficient condition for stability for all  $\tau$  is again  $\mu \geq 1$ .

In conclusion we recall that  $\mu$  are the eigenvalues of the associated eigenproblem for the eigenfunctions in  $y$ , so that the above conditions should be satisfied by the smallest eigenvalue. Therefore when a numerical scheme is used also in  $y$ , or when interpolation is needed in  $x$ , the discrete analog of  $\hat{\mu}$  should be considered. In either the discrete or continuous case, stability can be guaranteed when  $\mu \geq 1$ . For the continuous case, with



$v = 0$  at the endpoints, all eigenvalues are greater than or equal to 1. The smallest eigenvalue for a discrete approximation to the operator  $(f^2 - \partial_y^2)$  can be guaranteed to be greater than one with a little care in the discretization of the coriolis term,  $f^2$ . For example, on an equatorial  $\beta$  plane with a uniform grid with grid size of  $\Delta y$ , and the second-order approximation to  $\partial_y^2$  given by

$$\partial_y^2 v \approx \delta_{yy} v = \frac{1}{\Delta y^2} (v_{i,j+1} - 2v_{i,j} + v_{i,j-1}),$$

the  $y$  grid should be arranged so that the equator (a zero of  $f$ ) lies half-way between grid points with the analytic operator  $f^2 = y^2$  being approximated as  $(y_j)^2$ . Using the Courant–Fischer minimax theorem (see Golub and VanLoan 1989), the smallest eigenvalue,  $\lambda_{\min}$  of a symmetric  $n \times n$  matrix,  $\mathbf{A}$ , can be written as

$$\lambda_{\min}(\mathbf{A}) = \min_{0 \neq x \in \mathbb{R}^n} \frac{x^T \mathbf{A} x}{x^T x}.$$

Therefore, for any two symmetric matrices,  $\mathbf{A}$  and  $\mathbf{B}$ ,

$$\begin{aligned} \lambda_{\min}(\mathbf{A} + \mathbf{B}) &= \min_{x \neq 0} \frac{x^T (\mathbf{A} + \mathbf{B}) x}{x^T x} \\ &\geq \min_{x \neq 0} \frac{x^T \mathbf{A} x}{x^T x} + \min_{z \neq 0} \frac{z^T \mathbf{B} z}{z^T z} \\ &= \lambda_{\min}(\mathbf{A}) + \lambda_{\min}(\mathbf{B}). \end{aligned}$$

The discrete operator  $-\delta_{yy}$  can be written as a symmetric tridiagonal matrix  $\mathbf{A}$  and  $f^2$  can be written as a diagonal matrix  $\mathbf{B}$ . The smallest eigenvalue of  $\mathbf{A}$  is given by

$$\lambda_{\min}(\mathbf{A}) = \frac{4}{\Delta y^2} \sin^2\left(\frac{\Delta y}{2}\right)$$

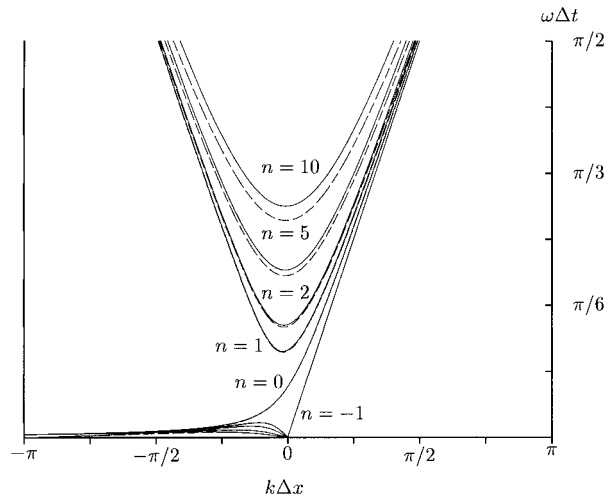
and the smallest eigenvalue of  $\mathbf{B}$  is given by

$$\lambda_{\min}(\mathbf{B}) = \left(\frac{\Delta y}{2}\right)^2.$$

The lower bound on  $\mu$  for the discrete operator then follows, since

$$\lambda_{\min}(\mathbf{A} + \mathbf{B}) \geq \left[1 - \frac{1}{3} \left(\frac{\Delta y}{2}\right)^2\right] + \left(\frac{\Delta y}{2}\right)^2 > 1.$$

A comparison of the analytic dispersion diagrams to the discrete dispersion diagrams for the special case of an equatorial  $\beta$  plane ( $f = y$ ) gives a good indication of the spatial and temporal accuracy constraints appropriate for the dynamics of interest. In Fig. 1 we plot the curves for a few values of the wavenumber  $n$  for the special case,  $\Delta t = \Delta x = 0.2$ . For this relatively fine resolution, there is very good agreement between the analytic and discrete curves for the Rossby waves of moderate wavenumber in  $x$  (see lower panel) and even for the gravity waves (upper portion of upper panel). For the equatorial Kelvin wave,  $n = -1$ , the curves are



discrete(dashed) vs. analytic(solid),  $\Delta t = 0.2$

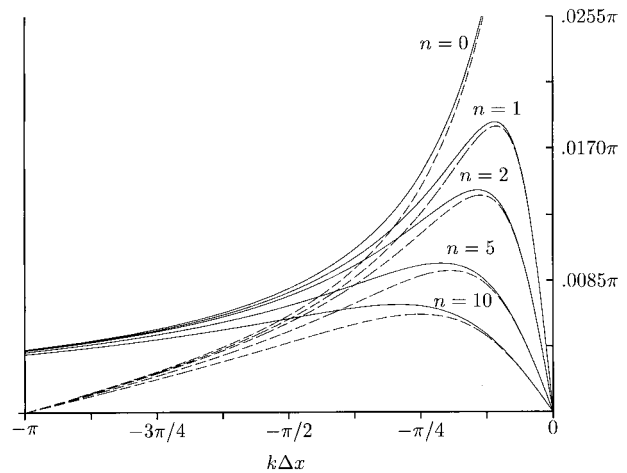
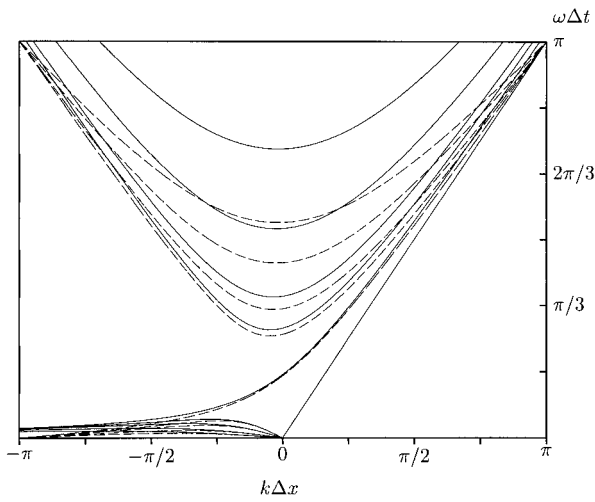


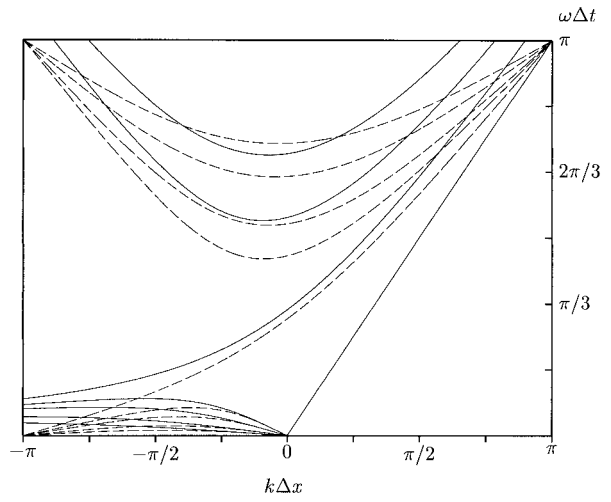
FIG. 1. Dispersion diagrams for  $\Delta t = 0.2$ .

identical and the curves for the Yanai, or mixed mode,  $n = 0$ , are almost identical. Note that, in these plots,  $\omega \Delta t = \pi$  and  $k \Delta x = \pi$  correspond to the highest frequency represented on the grids, that is, the two grid-point wave.

For larger time steps, there is a greater discrepancy between the discrete and analytic curves, see Figs. 2 and 3, but they are arguably close enough for most climate-scale ocean dynamics. (For a fast baroclinic mode in the ocean with a grid spacing of  $\Delta x = 1/2$ , or  $1.6^\circ$ , a wavenumber of  $\pi/4$  corresponds to a wavelength of about 1200 km and  $\Delta t = 1/2$  corresponds to about 18 h.) For  $\Delta t = 2$ , the curves are close only for the Rossby waves with very small  $k$  and even for these the maxima of the curves (distinguishing regions of eastward and westward propagation of energy) are way off, see Fig. 4. In the following section we explore the effect of this



discrete(dashed) vs. analytic(solid),  $\Delta t = 0.5$



discrete(dashed) vs. analytic(solid),  $\Delta t = 1.0$

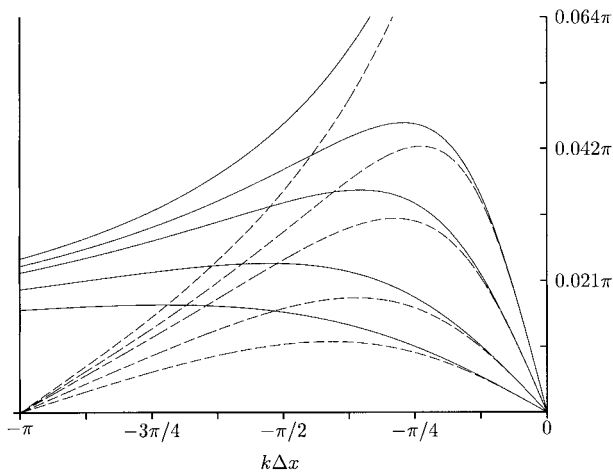


FIG. 2. Dispersion diagrams for  $\Delta t = 0.5$ .

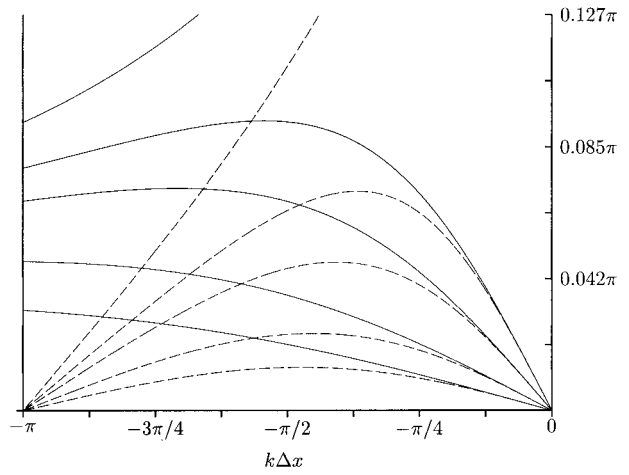


FIG. 3. Dispersion diagrams for  $\Delta t = 1.0$ .

discretization error for the time and length scales relative to the fastest baroclinic (internal) modes of the ocean.

**6. Experiments**

In this section we illustrate the stability and accuracy of the INC scheme for time and length scales appropriate to ocean dynamics with a few simple experiments.

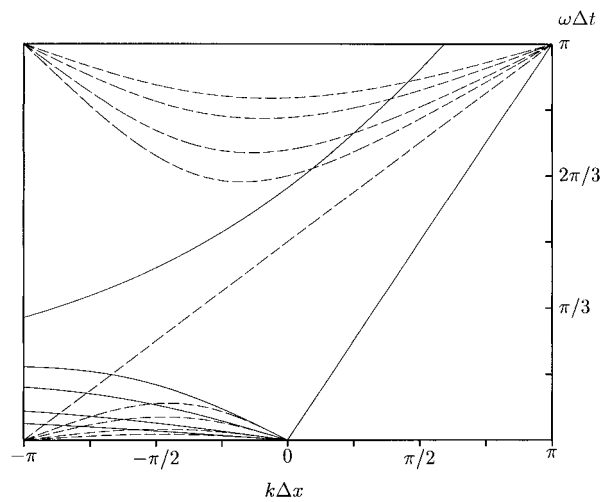
*a. Midlatitude Gaussian bump—Periodic domain*

A midlatitude Gaussian perturbation of  $h$  is allowed to propagate in a semiperiodic domain, from  $20^\circ\text{N}$  to  $60^\circ\text{N}$  on a  $90^\circ$  wide beta plane centered at  $40^\circ\text{N}$ . We assume an internal wave speed of  $3.17 \text{ m s}^{-1}$ , corresponding to a horizontal scale  $L \approx 425 \text{ km}$ .

In the meridional direction, we use a relatively high resolution of  $1/4^\circ$  (scaled,  $\Delta y = 0.05$ ) so that errors due to the discretization in  $y$  will be negligible compared with those in  $x$  and  $t$ . The zonal and time resolutions are varied. A scaled  $\Delta x = 1$  corresponds to a  $5^\circ$  zonal resolution and a scaled  $\Delta t = 1$  corresponds to a time step of 37.3 h.

In this unforced initial value problem we expect the initial perturbation to propagate westward. Because we are initializing with a Gaussian, we expect to see dispersion in the wake of the initial bump associated with the higher frequency waves.

Figures 5 and 6 show plots of the propagation of the anomaly at 2-year intervals, for various values of  $\Delta t$  and  $\Delta x$ . The actual solution is shown in Fig. 5a (obtained by the leapfrog method, checking for convergence by successively reducing  $\Delta x$ ,  $\Delta y$ , and  $\Delta t$ ).



discrete(dashed) vs. analytic(solid),  $\Delta t = 2.0$

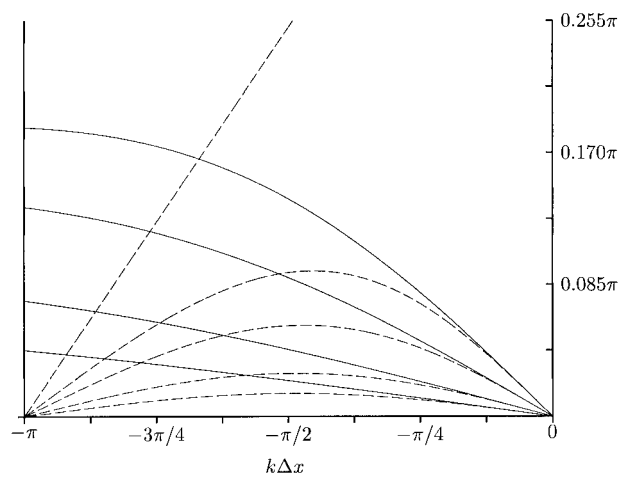


FIG. 4. Dispersion diagrams for  $\Delta t = 2.0$ .

Note that Figs. 5c and 6a are almost identical, showing again that it is time accuracy that dictates the overall accuracy at these resolutions. Figure 6c shows the dispersive nature of the scheme for a larger time step,  $\Delta t = 1$ , as expected from the dispersion diagram in Fig. 3. All of the above experiments were with  $\Delta t$  an integer multiple of  $\Delta x$ , so that take-off points always correspond to grid points. When  $\Delta t$  is not an integer multiple of  $\Delta x$ , diffusion is introduced due to the interpolation of values from grid points to take-off points. This diffusion is largest for the case where  $\Delta x = 2\Delta t$ , where take-off points are half-way between grid points (see Fig. 6b).

*b. Midlatitude Gaussian bump—Bounded domain*

When we introduce eastern and western boundaries, we expect a more complicated sequence of events. The

initial westward propagation of the Northern Hemisphere perturbation continues until it hits the western boundary. This creates a coastal Kelvin wave propagating equatorward. An equatorial Kelvin wave carries the perturbation eastward along the equator. Then Rossby waves spread the perturbation slowly back into the domain from the eastern boundary in the characteristic parabolic shape, propagating faster at lower latitudes, slower at higher latitudes. We illustrate the correct modeling of this behavior by the INC scheme using the Atlantic Basin, artificially closed at  $30^\circ\text{S}$  and  $60^\circ\text{N}$ . In Fig. 7, the perturbation is shown at monthly intervals, from left to right, continued on the line below.

*c. Forced motion, equatorial Pacific*

Finally, we test the new INC scheme in our domain of primary interest, the equatorial Pacific. We first compare the INC scheme to both the CP and leapfrog (LF) schemes for a simplified equatorial Pacific basin. For a typical equatorial Pacific density structure, the first baroclinic mode has an equivalent depth of 84 cm, Kelvin wave speed of  $287 \text{ cm s}^{-1}$ , horizontal length scale of  $3.19^\circ$ , and timescale of 1.43 days. We force this mode with the Florida State University analysis (Legler and O'Brien) of monthly wind stress anomalies from 1964 to 1991. Due to constraints of the CP methodology, we approximate the basin geometry, representing Australia and North America by rectangular regions in the southwest and northeast corners, respectively. All three schemes were run on a  $2^\circ$  by  $\frac{1}{2}^\circ$  grid. The finer meridional resolution is required to resolve the equatorial dynamics. The CP scheme is run with a time step of 5 days and the LF a time step of 2 h. For the INC scheme, we have seen that the zonal resolution dictates a natural time step, for which the scaled value of  $\Delta t$  equals the scaled value of  $\Delta x$ . Since  $\Delta x = 2^\circ/3.19^\circ \approx 0.627$ , this implies a time step of approximately 22 h. The anomalous pressures at the end of 1991, computed by the CP, LF, and INC schemes are shown in Figs. 8a–c, respectively. The solutions are in close agreement near the equator and in the interior, and differ near boundaries, due to varying boundary treatment. In Figs. 9a,b, we also show the INC solution using time steps of a half and a full CP time step of 5 days. Clearly the INC scheme solution is not very accurate at the CP time step, but the 2.5 day time step solution is better. The time step of the LF scheme is limited by the CFL restriction imposed by the high resolution in the meridional direction. In addition, near the western boundary, the LF scheme also requires the addition of a small amount of horizontal diffusion. In this case we use a diffusion (Laplacian) coefficient of  $2 \times 10^2 \text{ m}^2 \text{ s}^{-1}$  in the meridional direction, and  $2 \times 10^3 \text{ m}^2 \text{ s}^{-1}$  in the zonal direction.

Although the CP scheme has the advantage of the larger time step, it is limited to simple geometries. The INC scheme is not, and we illustrate the results of re-



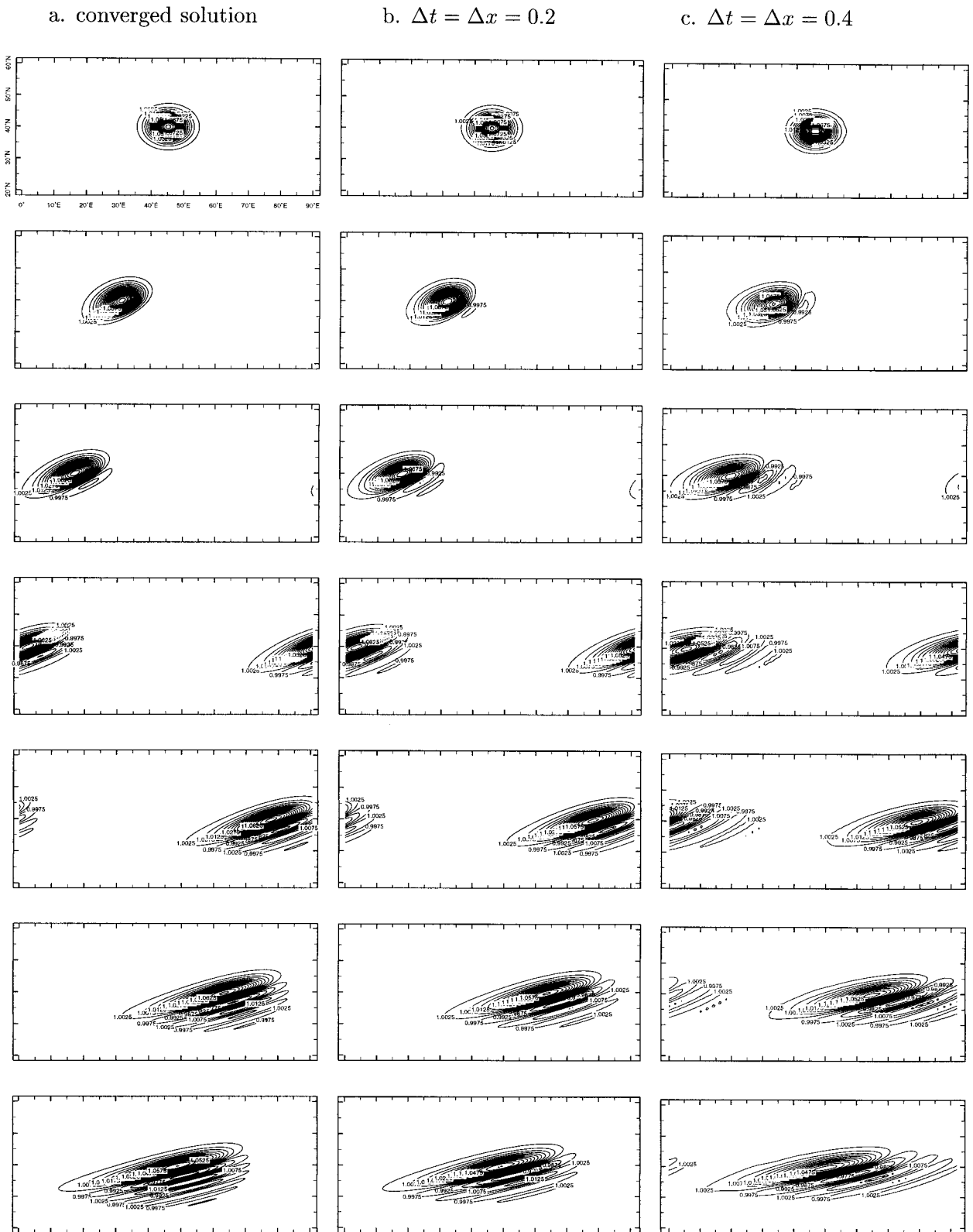


FIG. 5. Propagation of a midlatitude depth perturbation in a periodic domain.

a.  $\Delta t = 0.4, \Delta x = 0.2$

b.  $\Delta t = 0.2, \Delta x = 0.4$

c.  $\Delta t = \Delta x = 1.0$

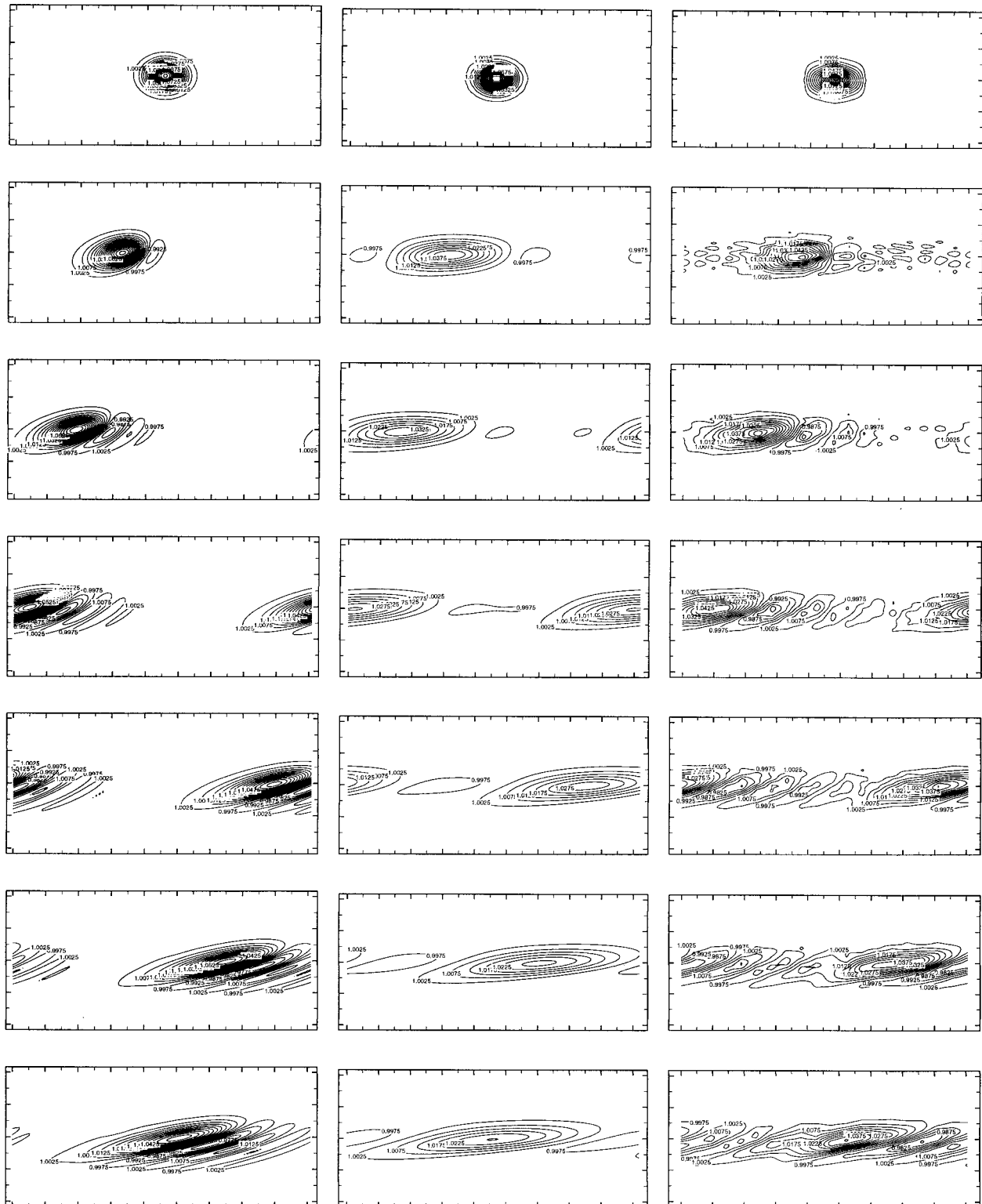


FIG. 6. Propagation of a midlatitude depth perturbation in a periodic domain,  $\Delta t = 1$ .

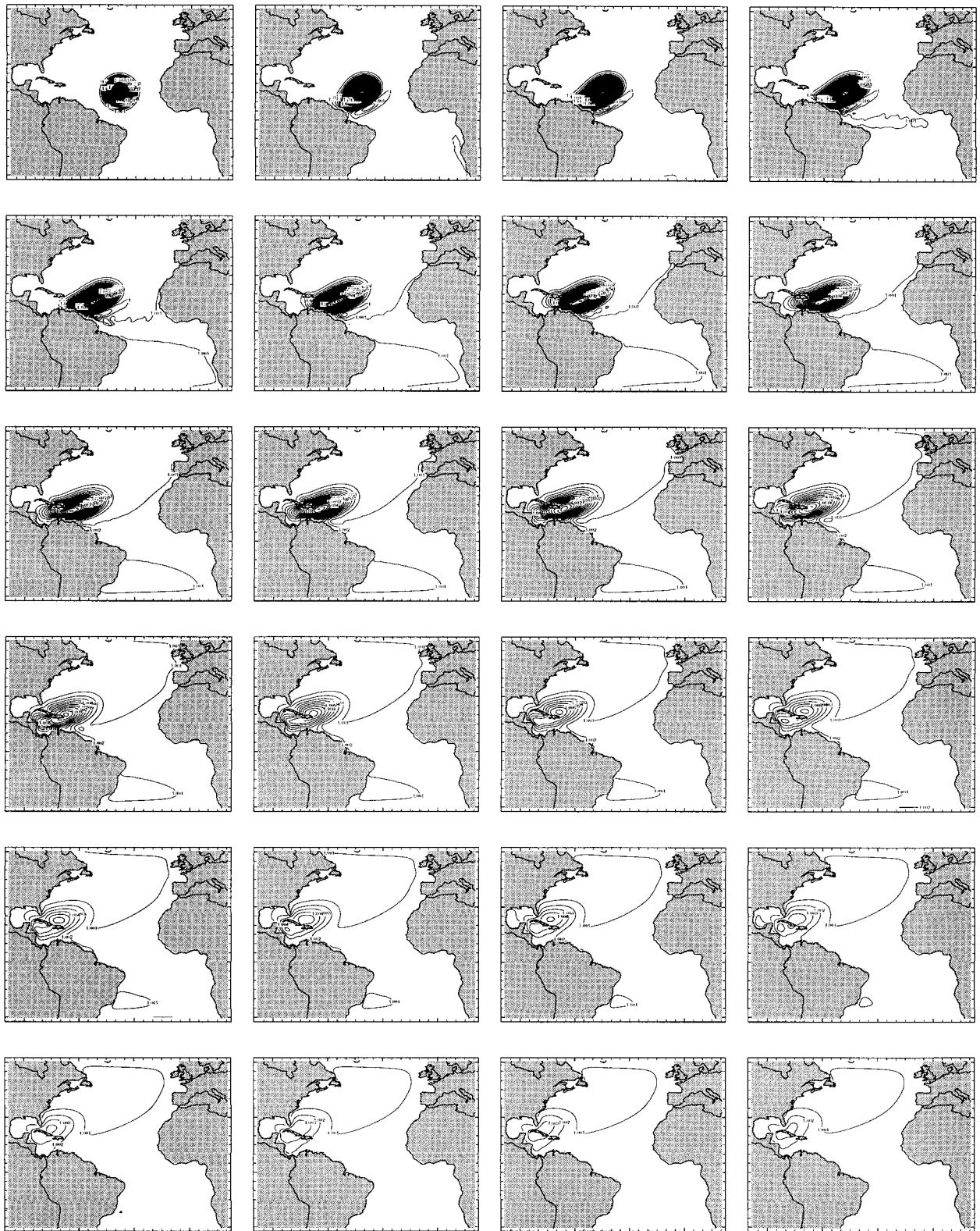


FIG. 7. Propagation of a depth perturbation in the North Atlantic.



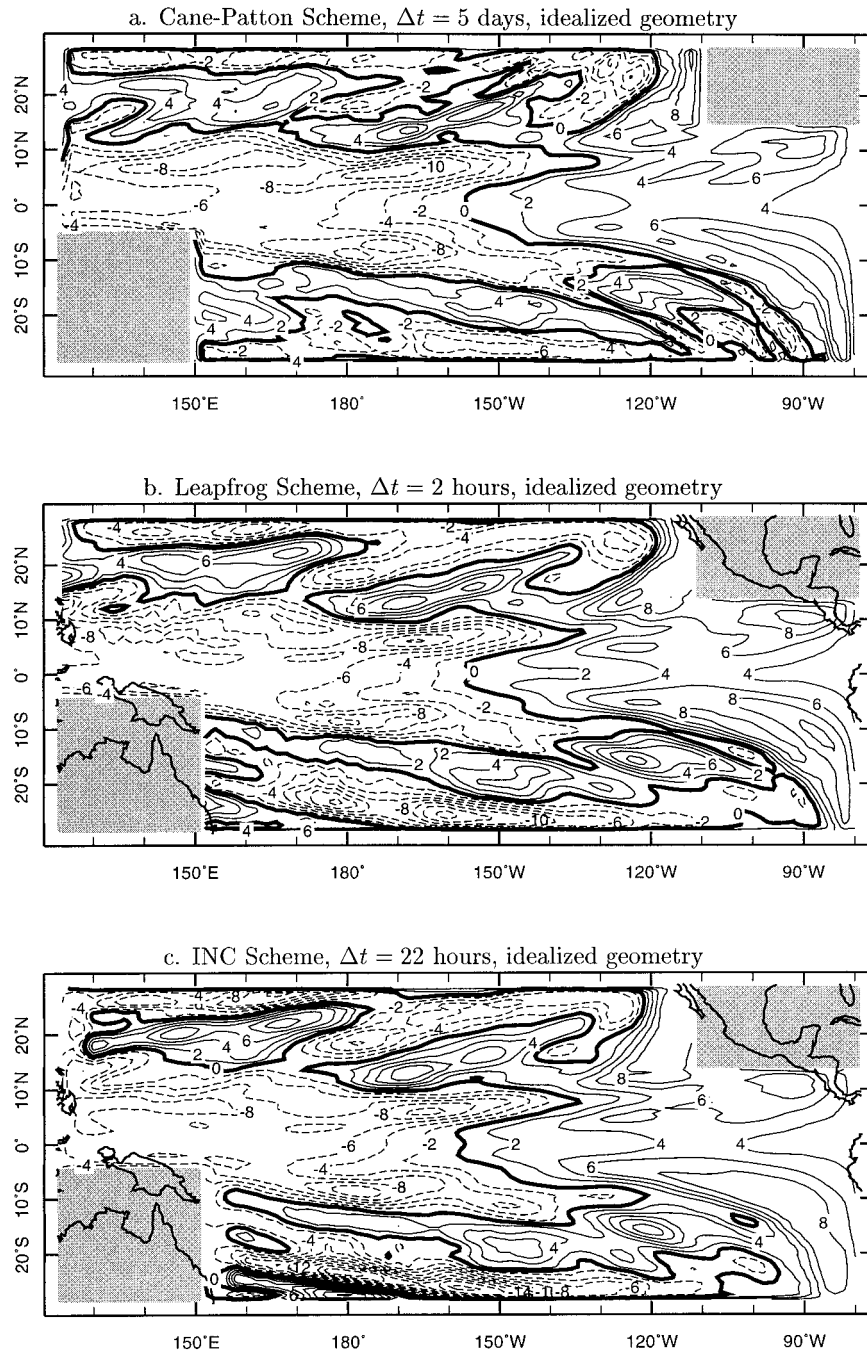


FIG. 8. Comparison of CP, leapfrog, and INC schemes in the equatorial Pacific.

peating the above experiment in a basin with more realistic geometry. The final anomalous pressure field is shown in Fig. 9c.

**7. Conclusions**

The existing schemes for solving the shallow water equations to which INC should be compared fall into two major categories, explicit and implicit in time. The

efficiency of explicit schemes are limited by the CFL conditions and require time steps on the order of an hour for the fastest baroclinic mode. The CFL is imposed by gravity waves, and this time step is an order of magnitude smaller than typically needed for the accurate computation of Rossby waves. The only constraint on the time step of the INC scheme arises from accuracy considerations, which may allow an order of magnitude improvement in efficiency. The other implicit

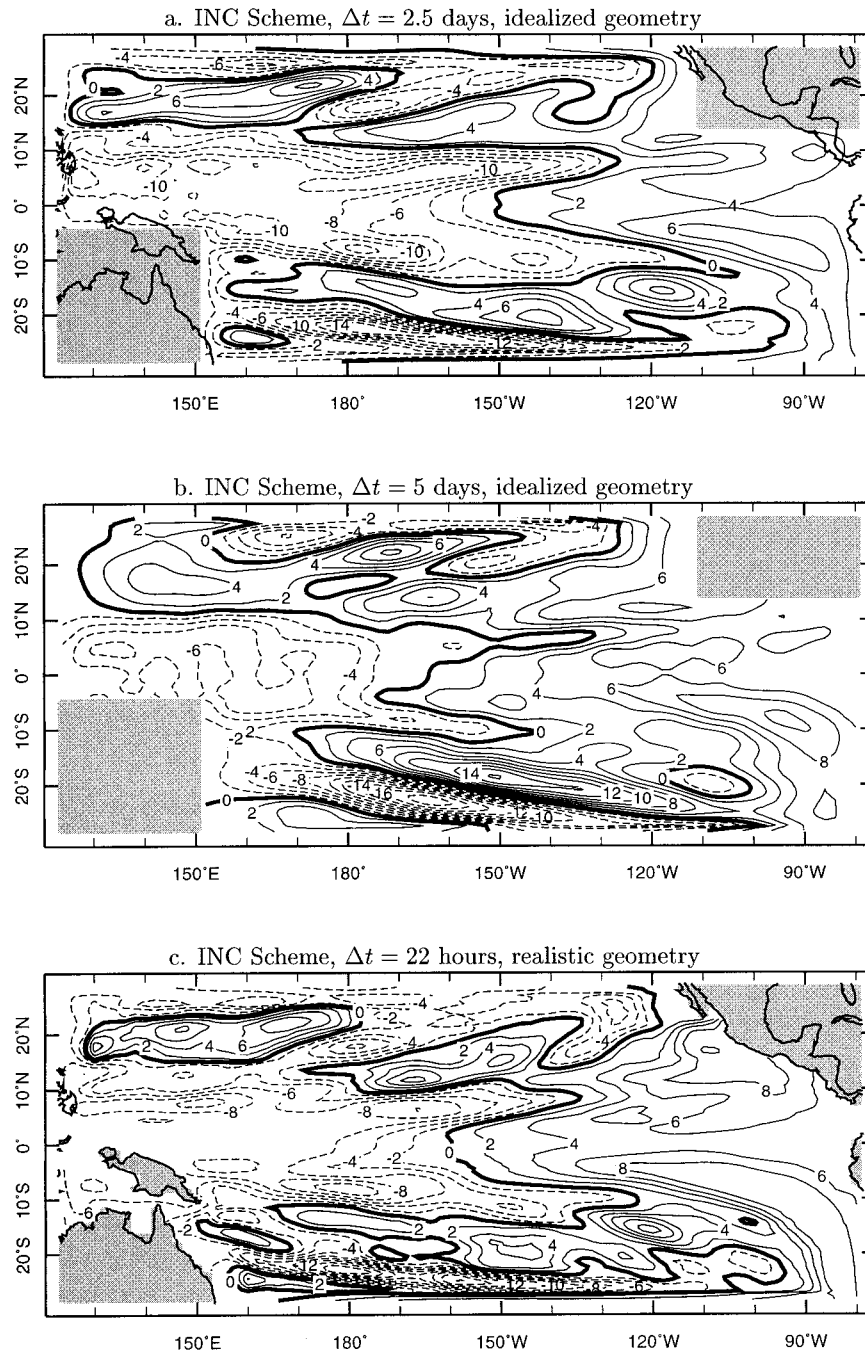


FIG. 9. Comparison of INC solutions using a long time step and a more realistic equatorial Pacific.

schemes (semiimplicit/semi-Lagrangian, fully implicit) usually require more work (either for the interpolations, or for the solution of very large linear systems) in exchange for an increase in the time step, often with little

or no net gain in efficiency. The INC scheme, by decoupling the zonal and meridional dependencies, retains the per time step efficiency of the explicit schemes, while eliminating the CFL restriction on the size of the



time step. As can be seen from the analysis and some simple experiments presented here, the time step is constrained by zonal accuracy considerations.

Thus we conclude that the INC scheme is an efficient alternative to the standard schemes, giving an order of magnitude in speed with little loss in accuracy. Moreover, INC can be used for the wave solve of more general systems such as those with nonlinearities and used in semi-Lagrangian and semiimplicit schemes.

*Acknowledgments.* This work was supported by NOAA Grant UCSIO-10075411, NASA Grant NAG5-6315, and the generous support of the Vetlesen Foundation.

APPENDIX  
Near-Boundary Formulas

If  $\Delta t > \Delta x$ , characteristics may intersect a boundary in the time interval  $(t, t + \Delta t)$ . This occurs at all grid

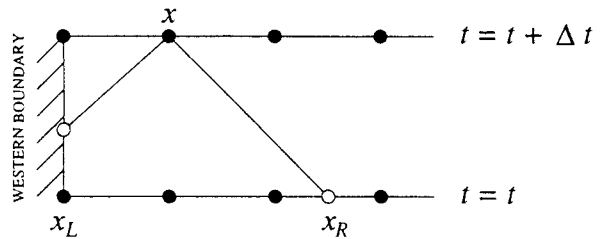


FIG. A1. Schematic of characteristic intersecting the western boundary.

points that are within a distance  $\Delta t$  of an “ $x$ -boundary.” For this case, the length of the path of integration along the left and right characteristics, must be reduced. See Fig. A1, where the left characteristic intersects the western boundary.

The general equations can be written as

$$\begin{aligned} (u + h)^{n+1} &= (u + h)_L^n + \tau_L[(fv - \partial_y v + F + Q)^{n+1} + (fv - \partial_y v + F + Q)_L^n] \\ (u - h)^{n+1} &= (u - h)_R^n + \tau_R[(fv - \partial_y v + F - Q)^{n+1} + (fv + \partial_y v + F - Q)_R^n] \\ v^{n+1} - v^n + \tau(\partial_y h^{n+1} + \partial_y h^n + fu^{n+1} + fu^n) &= \tau(G^{n+1} + G^n), \end{aligned}$$

where

$$\tau_L = |x - x_L|/2 \quad \tau_R = |x - x_R|/2.$$

Note that quantities evaluated at the boundary are at an intermediate time. These quantities are obtained by a constant extrapolation in time.

The algorithm can now be rewritten as the following.

Modified time-stepping algorithm—Interior points

1M. Find  $c^n$  and  $d^n$ :

$$\begin{aligned} c^n &= \frac{1}{2}(I_1 + I_2) + \bar{\tau}F + \tau'Q, \\ I_1 &= (u + h)_L^n + \tau_L(fv - \partial_y v + F + Q)_L^n \\ d^n &= \frac{1}{2}(I_1 - I_2) + \tau'F + \bar{\tau}Q, \\ I_2 &= (u - h)_R^n + \tau_R(fv + \partial_y v + F - Q)_R^n. \end{aligned}$$

2M. Find  $v = v^{n+1}$  by solving an ODE in  $y$  for each value of  $x$ :

$$\begin{aligned} \partial_y^2 v - \left( f^2 + \frac{1}{\tau\bar{\tau}} + \frac{\tau'}{\bar{\tau}} \right) v &= \frac{1}{\bar{\tau}}[fu^n + fc^n + \partial_y(h^n + d^n) - (G + G^n)] \\ &\quad - \frac{1}{\tau\bar{\tau}}v^n. \end{aligned}$$

4M. Find  $u = u^{n+1}$  and  $h = h^{n+1}$ :

$$\begin{aligned} u &= \bar{\tau}fv - \tau'\partial_y v + c^n & h &= \tau'fv - \bar{\tau}\partial_y v + d^n, \\ \text{where } \bar{\tau} &= (\tau_R + \tau_L)/2 & \text{and } \tau' &= (\tau_L - \tau_R)/2. \end{aligned}$$

REFERENCES

Cane, M. A., and E. S. Sarachik, 1979: Forced baroclinic ocean motion. Part III: An enclosed ocean. *J. Mar. Res.*, **37**, 355–398.  
 —, and R. J. Patton, 1984: A numerical model for low-frequency equatorial dynamics. *J. Phys. Oceanogr.*, **14**, 1853–1863.  
 Golub, G. H., and C. F. Van Loan, 1989: *Matrix Computations*. 2d ed. The Johns Hopkins University Press, 642 pp.  
 Roe, P., 1994: Linear bicharacteristic schemes without dissipation. ICASE Tech. Rep. 94-65, pp. [Available from Institute for Computer Applications in Science and Engineering, Mail Stop 32C, NASA LARC, Hampton, VA 23681-0001.]  
 Staniforth, A., and J. Côté, 1991: Semi-Lagrangian integration schemes for atmospheric models—A review. *Mon. Wea. Rev.*, **119**, 2206–2223.